

Characterization of a reduced molybdenum-oxo compound derived from an oxo-transfer process under stoichiometric conditions

Henri Arzoumanian^{a,*}, Robert Bakhtchadjian^a, Reinaldo Atencio^b,
Alexander Briceno^b, Gabriel Verde^b, Giuseppe Agrifoglio^{b,**}

^a UMR 6180 du CNRS, Université Aix-Marseille III, Faculté des Sciences St Jérôme, Avenue Escadrille Normandie Niemen, 13397 Marseille, France

^b Centro de Química, Instituto Venezolano de Investigaciones Científicas, Caracas, Venezuela

Received 10 May 2006; accepted 4 July 2006

Available online 22 August 2006

Abstract

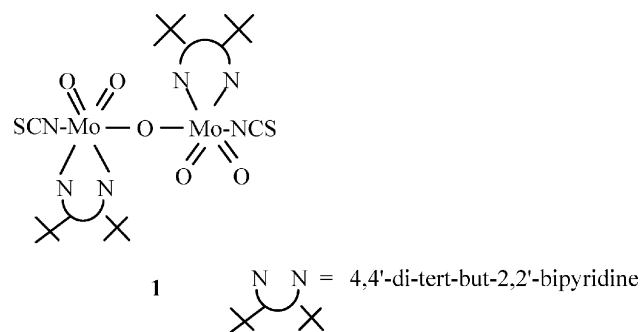
The stoichiometric oxidation of phosphanes or alcohols by a Mo(VI)-dioxo complex (**1**) followed both by UV spectroscopy results in the formation of a Mo(V) dimer with two μ -oxo bridges and two terminal oxo functions (**3**). Its structure is determined by an X-ray analysis depicting a Mo–Mo bond well in accord with the diamagnetic character of the complex. The spectroscopic follow up of the oxygen atom transfer process shows clearly that complex **3** is the end product of a series of intermediates among which one (**2**) is postulated as being a geometrical isomer of **3**. © 2006 Elsevier B.V. All rights reserved.

Keywords: Oxygen atom transfer; Molybdenum-dioxo; UV spectroscopy

1. Introduction

Numerous transition metal oxo-transfer systems have been studied, either as enzymatic oxo-transferase models or in the pursuit of efficient catalytic oxidation processes [1]. In the majority of cases, the characterization of the species responsible for the oxygen atom transfer to the substrate is well established. On the other hand, the exact nature of the reduced entity, arisen from this transfer is, with some exceptions [2,3], often ill-defined and at best is based on spectroscopic evidence on final products. Very rare are the examples of studies in which specific attention was given to the end-reduced species.

We have been studying various molybdenum and tungsten-oxo complexes capable of transferring oxo moieties to various substrates [1d,4]. Recently, we investigated more in details a molybdenum(VI)-dioxo compound (**1**) that had shown exceptional catalytic oxo-transfer capabilities [5]. It is a μ -oxo dimer bearing thiocyanato groups and a bulky 4,4'-di-*tert*-butyl-2,2'-bipyridyl ligands,



The present report concerns the isolation and characterization of the reduced molybdenum compound obtained upon the oxygen atom transfer from **1** to phosphanes or alcohols under stoichiometric conditions.

2. Experimental

2.1. General

All materials were commercial products and were used without further purifications unless otherwise noted. All solvents were thoroughly degassed prior to use by repeated evacuation followed by admission of dry and oxygen free nitrogen

* Corresponding author. Tel.: +33 491288256; fax: +33 491289146.

** Corresponding author.

E-mail addresses: henri.arzoumanian@univ.u-3mrs.fr (H. Arzoumanian), gagrifog@cantv.net (G. Agrifoglio).

or argon. Dichloromethane and *n*-hexane were dried over activated molecular sieves. Complex **1** was prepared as reported [5]. Triphenylphosphane was recrystallized prior to use and checked by ^{31}P NMR for purity. IR spectra were recorded on a Perkin-Elmer 1720 XFT spectrometer. UV spectra were recorded on a Hewlett Packard 8453 diode array spectrometer. ^1H , ^{13}C , ^{31}P NMR spectra were recorded on Bruker 300 and 500 (Avance) spectrometers.

2.2. Synthesis of **3**

To a degassed dichloromethane solution (50 mL) containing triphenylphosphane (176 mg, 6.6 mmol), was added at 25 °C and under argon, 66 mg (0.66 mmol) of **1**. The purple coloration immediately observed intensified with time to nearly blue-black and then slowly lightened. The mixture was stirred overnight and evaporated under vacuum. The residue was washed repeatedly ($\times 3$) with *n*-hexane and diethyl ether to extract the excess triphenylphosphane and the triphenylphosphine oxide formed. The remaining solid was then crystallized in an acetonitrile/*n*-hexane (1/1) mixture to yield orange yellow crystalline **3**. M.p. > 250 °C. [(4,4'-*t*-bu-2,2'-bipy)Mo(O)(μO)NCS] $_2$ -CH $_3$ CN, C $_{40}$ H $_{51}$ N $_7$ O $_4$ S $_2$ Mo (948.9): calcd. C 50.57, H 5.41, N 10.32; found C 50.33, H 5.28, N 10.21. IR (KBr): $\nu = 2064\text{ cm}^{-1}$ (vs, νNCS), 958 (s, $\nu\text{Mo=O}$), 738 (m, $\nu\text{Mo-O}$). ^1H NMR (CD $_2$ Cl $_2$): $\delta = 9.64$ (d, $J = 6\text{ Hz}$, H α , H1 and H28), 7.17 (d, $J = 6\text{ Hz}$, H α , H10 and H19), 8.33 (d, $J = 1.2\text{ Hz}$, H γ), 8.12 (d, $J = 1.2\text{ Hz}$, H γ), 7.86 (dd, $J = 6\text{ Hz}$, 1.2 Hz, H β), 6.77 (dd, $J = 6\text{ Hz}$, 1.2 Hz, H β), 1.55 (s, *t*-Bu CH $_3$), 1.35 (s, *t*-Bu CH $_3$). ^{13}C NMR (CD $_2$ Cl $_2$): $\delta = 167.6, 165.7, 154.1, 152.4, 150.7, 149.5, 125.1, 122.9, 120.1, 119.1, 36.3, 35.9, 30.5, 30.4$.

The same procedure was followed for the oxidation of 2-ethoxyethanol.

Table 2

Selected bond lengths [Å] and angles [°] for compound **3**

Mo(1)–O(1)	1.682(3)	O(1)–Mo(1)–O(4)	112.52(15)
Mo(1)–O(4)	1.914(3)	O(1)–Mo(1)–O(3)	105.55(16)
Mo(1)–O(3)	1.929(3)	O(4)–Mo(1)–O(3)	92.15(14)
Mo(1)–Mo(2)	2.5541(9)	O(1)–Mo(1)–N(5)	89.35(17)
Mo(1)–N(5)	2.202(5)	O(4)–Mo(1)–N(5)	89.41(16)
Mo(1)–N(1)	2.218(4)	O(3)–Mo(1)–N(5)	163.07(16)
Mo(1)–N(2)	2.331(4)	O(1)–Mo(1)–N(1)	92.38(15)
N(5)–C(38)	1.108(7)	O(4)–Mo(1)–N(1)	155.06(14)
S(1)–C(38)	1.621(7)	O(3)–Mo(1)–N(1)	82.04(14)
Mo(2)–O(2)	1.679(3)	N(5)–Mo(1)–N(1)	89.48(16)
Mo(2)–O(3)	1.925(3)	O(1)–Mo(1)–N(2)	156.45(15)
Mo(2)–O(4)	1.943(3)	O(4)–Mo(1)–N(2)	85.75(14)
Mo(2)–N(6)	2.165(6)	O(3)–Mo(1)–N(2)	87.71(15)
Mo(2)–N(4)	2.231(4)	N(5)–Mo(1)–N(2)	75.59(16)
Mo(2)–N(3)	2.314(4)	N(1)–Mo(1)–N(2)	69.87(13)
N(6)–C(37)	1.091(7)	O(1)–Mo(1)–Mo(2)	100.01(12)
S(2)–C(37)	1.650(7)	O(4)–Mo(1)–Mo(2)	49.01(10)
		O(3)–Mo(1)–Mo(2)	48.43(10)
		N(5)–Mo(1)–Mo(2)	137.89(12)
		N(1)–Mo(1)–Mo(2)	130.47(11)
		N(2)–Mo(1)–Mo(2)	103.30(10)

2.3. X-ray crystallography

Experimental details of the X-ray analysis are provided in Tables 1 and 2. All diffraction data were collected on a Rigaku AFC7S diffractometer using the programs TEXSAN [6], SHELXS-97 [7], SHELXS-97 [8], for data reduction, structure solution and structure refinement. Refinement of F^2 was performed against all reflections. The weighed R -factors are based on F , with F set to zero for negative F^2 . Crystallographic data for the structure of **3** has been deposited with the Cambridge Crystallographic Center with the number CCDC 181127. Copies of the data can be obtained free of charge on application to CCDC, 12 Union Road, Cambridge CB2 1EZ, UK [Fax: (internet) +44 1223 336 033, e-mail: deposit@ccdc.cam.ac.uk].

3. Results and discussion

Thiocyanato molybdenum-dioxo and dioxo- μ -oxo compounds have been shown to oxidize readily phosphanes and alcohols, to give phosphine oxides and ketones or aldehydes, 200 times faster than other molybdenum-dioxo compounds such as dithiocarbamates. These highly efficient species have been studied mainly under catalytic conditions in the presence of oxygen atom donors such as DMSO, N $_2$ O or O $_2$ [9,10].

In the absence of such oxidizing agents one might expect to isolate and characterize the reduced molybdenum species formed after the oxygen atom transfer process. With this endeavour we reacted complex **1** stoichiometrically either with excess triphenyl phosphane or an alcohol such as 2-ethoxyethanol. Upon work up, a yellow orange crystalline solid (**3**) was obtained, exhibiting in infrared spectroscopy characteristic bands for both terminal (958 cm^{-1}) and μ -oxo (738 cm^{-1}) functions as well as thiocyanato (2064 cm^{-1}) and bipyridyl ligands [11].

The X-ray analysis of a suitable crystal, obtained from the reaction with triphenyl phosphane, confirmed these

Table 1
Crystallographic data, data collection parameters and refinement results

Empirical formula	C $_{40}$ H $_{51}$ Mo $_2$ N $_7$ O $_4$ S $_2$
Molecular mass	949.88
Temperature [K]	293(2)
Crystal system	Triclinic
Space group	<i>P</i> -1
<i>a</i> [Å]	13.074(3)
<i>b</i> [Å]	14.822(3)
<i>c</i> [Å]	11.820(2)
α [°]	93.182(16)
β [°]	93.996(18)
γ [°]	96.18(2)
Volume [Å 3]	2267.1(9)
<i>Z</i>	2
<i>D</i> $_c$ [g cm $^{-3}$]	1.391
Wavelength [Å]	0.71073 (Mo K α)
<i>F</i> (000)	976
Θ range [°]	1.57–25.01
Unique reflection with $I > 2\sigma(I)$	5816
Final <i>R</i> $_1$, <i>wR</i> $_2$ indices	0.0507, 0.1207
No. of variables	453
GOF	1.040

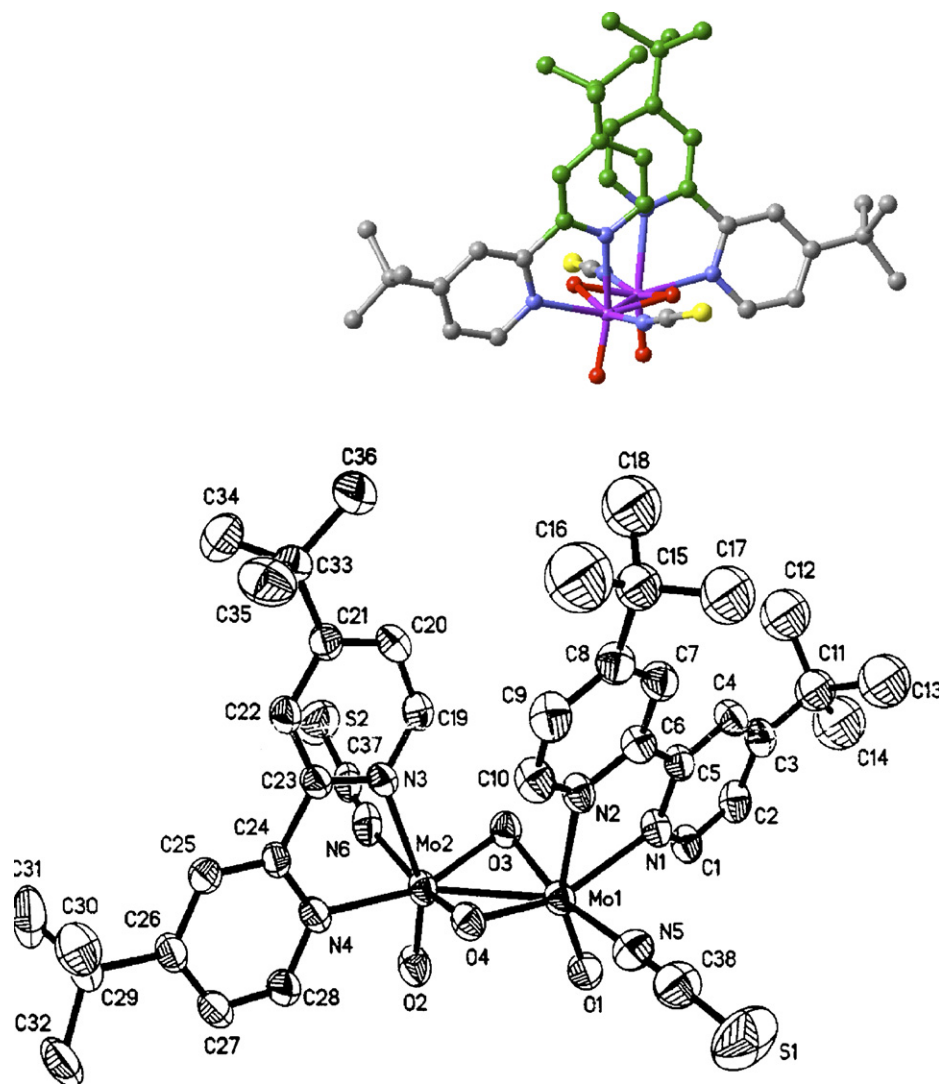
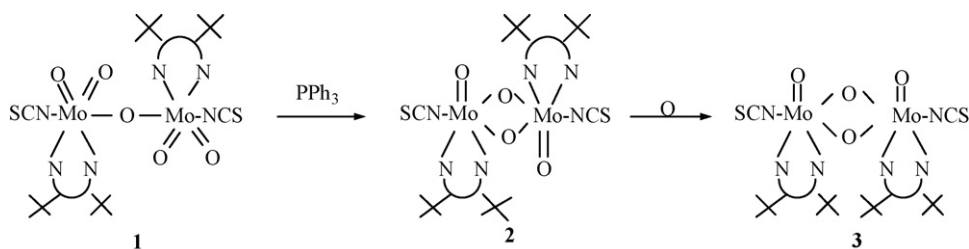


Fig. 1. ORTEP plot of complex **3** with atom-labeling scheme. Thermal ellipsoids drawn at the 35% probability level. Hydrogen atoms and solvent, CH_3CN are omitted for clarity. A different angle view in upper part shows the difference in environment for the two pyridyl rings of the bipy ligand.

observations. A view of complex **3** is depicted in Fig. 1 [12]. The experimental details of the analysis are given in Table 1 and the relevant bond lengths and bond angles are presented in Table 2. It depicts a molybdenum(V) dimer with two μ -oxo bridges and two terminal oxo functions placed in a *syn* position with the two thiocyanato groups lying *trans* to each other. The structural features for complex **3** compare favorably with related compounds [13,14]. The $\text{Mo}_2(\mu\text{-O})_2$ moiety is not planar with the center of the O3–O4 line at a point 0.41 Å from the center of the Mo–Mo line. This corresponds to a dihedral angle of 146.8° between the two $\text{Mo}(\mu\text{-O})_2$ planes, comparable with that on the $\text{Mo}_2\text{O}_4(\text{R-pdta})$ complex [15]. There is a slight twist in the central O1–Mo1–($\mu\text{-O}$)₂–Mo2–O2 group such that the O1=Mo1–Mo2=O2 chain has a torsional angle of 9.1°. The interaction of the Mo atoms with the terminal oxo ligands is manifested by a moderate *trans* influence with the Mo–N distances *cis* to the Mo=O terminal of 0.113 and 0.083 Å shorter than the *trans* Mo–N distances. The geometry about each molybdenum can be described as a distorted octahedron while the Mo–Mo distance is well within the limits of a metal–metal

single bond and explains the diamagnetic character of the Mo(V) species [16] verified by the NMR spectroscopic analysis. Indeed, the ^1H and ^{13}C NMR spectra of this complex exhibits two resonances for each bipyridine protons and carbons as well as two distinct *tert*-butyl signals indicating that the two pyridyl rings are not equivalent neither in solution nor in the solid state. A different angle view of the complex **3**, shown in the upper right part of Fig. 1, makes this interpretation more evident. Furthermore, not only the dissymmetry of the two pyridyl rings is explicit, but the interatomic distances between $\alpha\text{H}1$ and O1 or $\alpha\text{H}28$ and O2, respectively (2.56 Å) and $\alpha\text{H}10$ and O1 or $\alpha\text{H}19$ and O2 (4.84 Å) clearly justifies the unusually large difference in chemical shift ($\Delta = 2 \times 5$ ppm) of the two αH . The difference between the β and γ hydrogen atoms are understandably lesser.

When **1** reacts under catalytic conditions in the presence of oxygen atom donors, one can assume that the oxidation of the substrate is accompanied by the reduction of the molybdenum complex generating an entity capable of being reoxidized by the oxidizing agent. The high stability of **3** to air or even DMSO clearly indicates that it cannot be part of any catalytic



Scheme 1.

cycle and must be formed irreversibly and excluded from such a cycle.

It remains plausible, however, that a potentially active intermediate could be observed prior to the formation of **3**.

Absorption spectroscopy was the first tool used; it revealed several aspects of interest. Fig. 2 shows a scan spectrum of the reaction of **1** with an excess of triphenylphosphane in CH_2Cl_2 . Upon mixing solutions of **1** and PPh_3 under anaerobic conditions, the spectrum corresponding to **1** almost instantaneously disappears, while a greenish-blue coloration is briefly observed. Two absorption bands then appear, one at 567 nm which increases, reaches a maximum and then decreases, while a second at 431 nm increases steadily but at a slower rate. This is clearly seen in the absorbance versus time plot shown in the upper part of Fig. 2. All this is accompanied by the first appearance of a purple color and its slow disappearance to give at the end a yellowish solution. The features observed together with the changes in color seem related to those reported for $[\text{L}_2\text{Mo}_2\text{O}_4]^{2-}$ ions, in aqueous media, obtained by oxidation of Mo(III) compounds either in the *anti* or *syn* configuration [17,18]. In many examples, the thermodynamically less stable purple colored *anti* isomer (525–545 nm) is first formed followed by an isomerization to the yellow colored *syn* isomer (388–400 nm). It is thus feasible that an analogous reaction pathway, shown in Scheme 1, is operative in the case of the reduction of **1** by PPh_3 , the absorption at 567 nm corresponding to the purple *anti* isomer (**2**) and the weak absorption at 431 nm belonging to the yellow *syn* isomer (**3**) [19]. Recently, a theoretical study [20] on **1**, based on our experimental results, with Quantum Chemistry Parametric Method for Catalytic Reaction was reported. Conformational changes and/or loss of an oxo ligand was alternatively suggested for the reduction of one of the metallic centers to Mo(IV) followed by a comproportionation with the other Mo(VI) to yield the product (**3**).

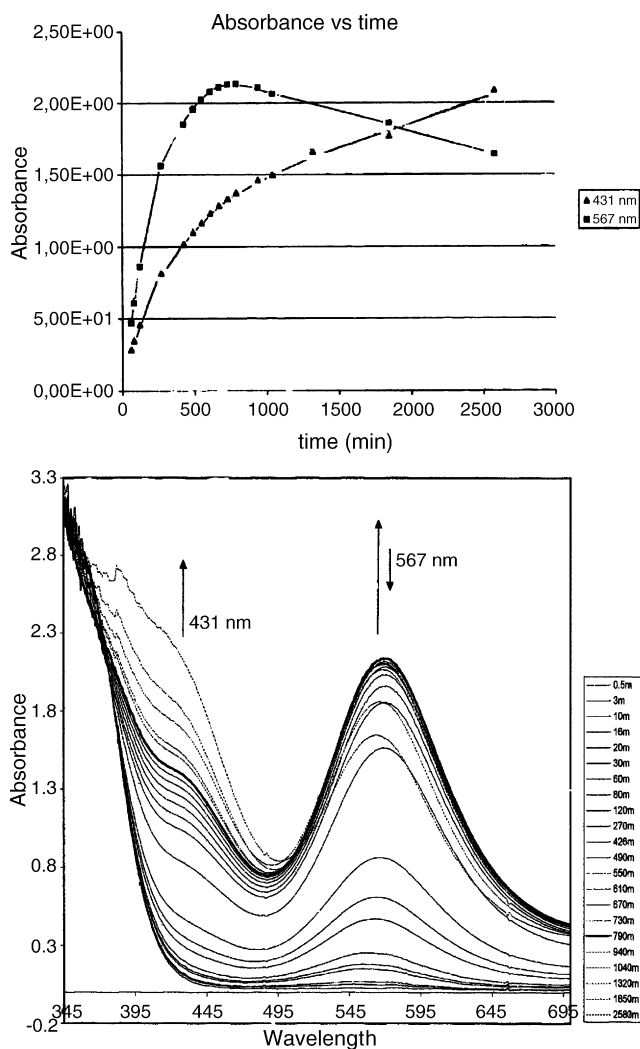


Fig. 2. Scan spectrum of the oxidation of triphenylphosphane by **1**. $[\mathbf{1}] = 0.44 \times 10^{-3} \text{ M}$; $[\text{PPh}_3] = 4.4 \times 10^{-3} \text{ M}$, in CH_2Cl_2 at 298 K. Absorbance vs. time plot shown in upper part.

neously disappears, while a greenish-blue coloration is briefly observed. Two absorption bands then appear, one at 567 nm which increases, reaches a maximum and then decreases, while a second at 431 nm increases steadily but at a slower rate. This is clearly seen in the absorbance versus time plot shown in the upper part of Fig. 2. All this is accompanied by the first appearance of a purple color and its slow disappearance to give at the end a yellowish solution. The features observed together with the changes in color seem related to those reported for $[\text{L}_2\text{Mo}_2\text{O}_4]^{2-}$ ions, in aqueous media, obtained by oxidation of Mo(III) compounds either in the *anti* or *syn* configuration [17,18]. In many examples, the thermodynamically less stable purple colored *anti* isomer (525–545 nm) is first formed followed by an isomerization to the yellow colored *syn* isomer (388–400 nm). It is thus feasible that an analogous reaction pathway, shown in Scheme 1, is operative in the case of the reduction of **1** by PPh_3 , the absorption at 567 nm corresponding to the purple *anti* isomer (**2**) and the weak absorption at 431 nm belonging to the yellow *syn* isomer (**3**) [19]. Recently, a theoretical study [20] on **1**, based on our experimental results, with Quantum Chemistry Parametric Method for Catalytic Reaction was reported. Conformational changes and/or loss of an oxo ligand was alternatively suggested for the reduction of one of the metallic centers to Mo(IV) followed by a comproportionation with the other Mo(VI) to yield the product (**3**).

4. Conclusion

We have investigated the oxygen atom transfer from a Mo-dioxo dimer complex (**1**) onto a phosphane or an alcohol and followed the process by UV spectroscopy. In all cases, the isolated end reduced product was a Mo(V) dimer (**3**) whose structure was established by an X-ray analysis. The spectroscopic analysis showed clearly the prior formation of the *anti* isomer (**2**) which rearranges to the more stable *syn* isomer (**3**). Although one cannot exclude the possibility of (**2**) being an intermediate in the catalytic cycle since it was not isolated and tested towards oxidation, its relative slow rate of formation suggests strongly that it, also, is formed irreversibly and then excluded from the catalytic cycle.

Acknowledgments

This work was performed under the auspices of the project ECOS Nord Venezuela No. V00P02 and project CONICIT S1-96001062, LAB-97000821, whose supports are kindly acknowledged. A.B. gratefully acknowledges CONICIT support. We

thank Dr. S. Pekerar for NMR assistance and Dr. M. Giorgi for X-ray contribution.

References

- [1] (a) R.H. Holm, *Chem. Rev.* (1987) 1401;
(b) F. Bottomley, L. Sutin, *Adv. Organomet. Chem.* 28 (1998) 339;
(c) R.H. Holm, *Coord. Chem. Rev.* 100 (1990) 183;
(d) H. Arzoumanian, *Coord. Chem. Rev.* 178–180 (Part 1) (1998) 191.
- [2] B.S. Lim, R.H. Holm, *J. Am. Chem. Soc.* 123 (2001) 1920.
- [3] K.-M. Sung, R.H. Holm, *J. Am. Chem. Soc.* 123 (2001) 1931.
- [4] H. Arzoumanian, G. Agrifoglio, M.V. Capparelli, R. Atencio, A. Briceño, A. Alvarez-Larena, *Inorg. Chim. Acta* 359 (2006) 81–89.
- [5] H. Arzoumanian, R. Bakhtchadjian, G. Agrifoglio, H. Krentzien, J.C. Daran, *Eur. J. Inorg. Chem.* (1999) 2225.
- [6] TEXSAN, Single Crystal Structure Analysis Software, Version 1.6, Molecular Structure Corporation, The Woodlands, TX 77381, USA, 1993.
- [7] G.M. Sheldrick, SHELXS97, Program for Crystal Structure Determination, University of Göttingen, Germany, 1997.
- [8] G.M. Sheldrick, SHELXS97, Program for Crystal Structure Refinement, University of Göttingen, Germany, 1997.
- [9] H. Arzoumanian, D. Nuel, J. Sanchez, *J. Mol. Catal.* 65 (1991) L9.
- [10] H. Arzoumanian, L. Maurino, G. Agrifoglio, *J. Mol. Catal. A: Chem.* 117 (1997) 471.
- [11] N.W. Nugent, J.M. Mayer, *Metal–Ligand Multiple Bonds*, Wiley, New York, 1998, pp. 113–119.
- [12] An X-ray analysis was also performed on the product obtained from the reaction with 2-ethoxyethanol. The structural features are identical, except for the presence of a ethoxyethanol molecule of crystallisation (all crystallographic data are available upon request). This is indicative of the general character as far as the formation of the end product.
- [13] J. Beck, W. Hiller, E. Scweda, J. Straehle, *Z. Naturforsch.* 39b (1984) 1110.
- [14] B.M. Gatehouse, E.K. Nunn, *Acta Cryst. Sect. B* 32 (1976) 1857.
- [15] A. Kojima, S. Ooi, Y. Sasaki, K.Z. Suzuki, K. Saito, H. Kuroya, *Bull. Chem. Soc. Jpn.* 54 (1981) 2457.
- [16] E.J. Stieffel, in: S.J. Lippard (Ed.), *Progress in Inorganic Chemistry*, vol. 22, Wiley, New York, 1997, p. 75.
- [17] M. Hahn, K. Wieghardt, *Inorg. Chem.* 23 (1984) 3977.
- [18] K. Wieghardt, M. Guttman, P. Chaudhuri, W. Gebert, M. Minelli, C.G. Young, J.H. Enemark, *Inorg. Chem.* 24 (1985) 3151.
- [19] The isomerisation step, shown in [Scheme 1](#), could plausibly be due to the presence of traces of water, as in the reported mechanism [14,15,21] or simply be the result of a spontaneous rearrangement. When the experiment was repeated in water-saturated CH₂Cl₂ only a very slight increase in rate was observed indicating that both water-catalyzed and spontaneous pathways could be operative.
- [20] B. Griffe, G. Agrifoglio, J. Britto, F. Ruetter, *Catal. Today* 107–108 (2005) 388.
- [21] S.E. Lincoln, T.M. Loehr, *Inorg. Chem.* 29 (1990) 1907.